Abnormal podocyte TRPML1 channel activity and exosome release in mice with podocyte-specific Asah1 gene deletion

Guangbi Li[a], **Dandan Huang**[a], **Owais M. Bhat**[a], **Justin L. Poklis**[a], **Aolin Zhang**[a], **Yao Zou**[a], **Jason Kidd**[b], **Todd W.B. Gehr**[b], **Pin-Lan Li**[a,*]

[a]Department of Pharmacology and Toxicology, School of Medicine, Virginia Commonwealth University, Richmond, VA, USA

[b]Division of Nephrology, School of Medicine, Virginia Commonwealth University, Richmond, VA, USA

Abstract

Podocytopathy and associated nephrotic syndrome (NS) have been reported in a knockout mouse strain (Asah1$^{fl/fl}$/Podo^{Cre}) with a podocyte-specific deletion of α subunit (the main catalytic subunit) of acid ceramidase (Ac). However, the pathogenesis of podocytopathy of these mice remains unknown. The present study tested whether exosome release from podocytes is enhanced due to Asah1 gene knockout, which may serve as a pathogenic mechanism switching on podocytopathy and associated NS in Asah1$^{fl/fl}$/Podo^{Cre} mice. We first demonstrated the remarkable elevation of urinary exosome excretion in Asah1$^{fl/fl}$/Podo^{Cre} mice compared with WT/WT mice, which was accompanied by significant Annexin-II (an exosome marker) accumulation in glomeruli of Asah1$^{fl/fl}$/Podo^{Cre} mice, as detected by immunohistochemistry. In cell studies, we also confirmed that Asah1 gene knockout enhanced exosome release in the primary cultures of podocyte isolated from Asah1$^{fl/fl}$/Podo^{Cre} mice compared to WT/WT mice. In the podocytes from Asah1$^{fl/fl}$/Podo^{Cre} mice, the interactions of lysosome and multivesicular body (MVB) were demonstrated to be decreased in comparison with those from their control littermates, suggesting reduced MVB degradation that may lead to increase in exosome release. Given the critical role of transient receptor potential mucolipin 1 (TRPML1) channel in Ca^{2+}-dependent lysosome trafficking and consequent lysosome-MVB interaction, we tested whether lysosomal Ca^{2+} release through TRPML1 channels is inhibited in the podocytes of Asah1$^{fl/fl}$/Podo^{Cre} mice. By GCaMP3 Ca^{2+} imaging, it was found that lysosomal Ca^{2+} release through TRPML1 channels was substantially suppressed in podocytes with Asah1 gene deletion. As an Ac

---

*Corresponding author at: Department of Pharmacology and Toxicology, Virginia Commonwealth University, School of Medicine, 1220 East Broad Street, Richmond, VA 23298-0613, USA. pin-lan.li@vcuhealth.org (P.-L. Li).

product, sphingosine was found to rescue TRPML1 channel activity and thereby recover lysosome-MVB interaction and reduce exosome release of podocytes from Asah1$^{fl/fl}$/Podo^{Cre} mice. Combination of *N, N*-dimethylsphingosine (DMS), a potent sphingosine kinase inhibitor, and sphingosine significantly inhibited urinary exosome excretion of Asah1$^{fl/fl}$/Podo^{Cre} mice. Moreover, rescue of Aash1 gene expression in podocytes of Asah1$^{fl/fl}$/Podo^{Cre} mice showed normal ceramide metabolism and exosome secretion. Based on these results, we conclude that the normal expression of Ac importantly contributes to the control of TRPML1 channel activity, lysosome-MVB interaction, and consequent exosome release from podocytes. Asah1 gene defect inhibits TRPML1 channel activity and thereby enhances exosome release, which may contribute to the development of podocytopathy and associated NS.

Keywords

Podocyte; Acid ceramidase; Exosome; Multivesicular body; Lysosome; TRPML1 channel

1. Introduction

As a regulator of cell-to-cell communication or signaling, extracellular vesicles (EVs) are now classified as three distinct populations including apoptotic bodies, microvesicles, and exosomes [1,2]. Exosomes, the smallest EV with approximately 50–140 nm in diameter, are formed through the endocytic process and released from intracellular multivesicular bodies (MVBs) through an active process [3]. In regard to the regulation of exosome release, lysosome function has been reported to determine the MVB fate through lysosome-dependent degradation of MVBs [4,5]. Pharmacological inhibition of lysosome function has been found to increase exosome secretion in different cells such as neurons, epithelial cells, and vascular cells [6-8]. Mechanistically, the regular trafficking of lysosomes may be essential for the fusion of lysosomes and MVBs, which is found to depend on lysosomal Ca^{2+} release [9-11]. Functionally, the exosome has been implicated in the pathogenesis of different diseases including renal and cardiovascular diseases [12-15]. Increasing evidence has shown that exosomes are not only an important biomarker for renal function or disease, but also serve as an critical mechanism mediating cell-to-cell communication in the kidney, which may participate in the development of various renal diseases [15-17]. Given the fact that podocytes can secret exosomes containing various factors [18,19] and that cellular function of podocytes is regulated by exosomes [17,20], the exosome secretion may be a crucial mechanism to turn on the podocyte dysfunction or injury leading to podocytopathy.

Podocytopathy is a critical pathological change which causes disruption of glomerular filtration barrier, proteinuria, and glomerular injury in the progression of end-stage renal disease. Despite extensive studies, however, the pathogenesis of podocytopathy remains poorly understood. Recently, we have demonstrated that podocyte-specific deletion of the α subunit (the main catalytic subunit) of acid ceramidase (Ac) leads to glomerular ceramide accumulation, proteinuria, and podocytopathy in a newly developed mouse strain (Asah1$^{fl/fl}$/Podo^{Cre}) [21]. Studies from our laboratory and by others have also demonstrated that increase in glomerular ceramide level importantly contributes to the development of glomerular disease under various pathological conditions [22]. Although these studies

defined the role of Ac-ceramide signaling in the development of podocytopathy, the precise mechanism mediating podocyte injury and initiating the nephrotic syndrome during Ac deficiency or gene deletion remains unclear. In this regard, earlier reports have shown that elevation of podocyte-derived exosome release is associated with albuminuria and glomerular degeneration in some patients with focal segmental glomerular sclerosis (FSGS) and nephrotic syndrome (NS) [15,23-25]. In diabetic mice, exosomes released from podocytes have been found to increase even before onset of albuminuria [18]. It has also been reported that lysosomal transient receptor potential mucolipin 1 (TRPML1) channel as a well-known lysosome function regulator is gated by Ac-associated sphingolipids, which is implicated in exosome release from podocytes [11]. These previous studies raised the possibility that Asah1 gene knockout may enhance exosome secretion from podocytes resulting in podocytopathy and NS due to TRPML1 channel dysfunction.

In the present study, we tested the hypothesis that Asah1 gene knockout in podocytes will result in the dysregulation of TRPML1 channel activity and thereby enhance exosome release, which may be a fundamental mechanism to cause podocytopathy and associated NS. To test this hypothesis, we first examined whether exosome release from podocytes is enhanced by Asah1 gene knockout in vivo and in vitro. Then, we determined the effect of Asah1 gene deletion on the lysosome-MVB interaction in podocytes and the role of TRPML1 channel in increased exosome secretion from podocytes with deficient Ac activity. Finally, we tested whether exogenous administration of an Ac product, sphingosine can recover the podocyte TRPML1 channel activity and enhance the interaction of lysosome and MVB, reducing exosome secretion. Our results demonstrate that a normal expression Asah1 gene is essential for the control of TRPML1 channel activity in podocytes and thus determines the fate of MVBs and consequent exosome release. Defect of this gene will lead to enhancement of exosome release from podocytes, which may be a novel mechanism switching on podocytopathy and NS.

2. Materials and methods

2.1. Animals

Metabolic cage experiments were performed to collect urine of eight-week-old WT/WT (C57BL/6 J) and Asah1^{fl/fl}/Podo[cre] mice [21]. Then, these mice were sacrificed and their kidneys were harvested for immunohistochemistry. In animal treatment experiments, eight-week-old WT/WT and Asah1^{fl/fl}/Podo[cre] mice received daily i.p. injection of *N*, *N*-dimethylsphingosine (Cayman Chemical, Ann Arbor, MI, USA) at 400 μg/kg [26] or combination of *N*, *N*-dimethylsphingosine and sphingosine (Cayman Chemical, Ann Arbor, MI, USA) at 8 mg/kg [27] for 2 weeks. After treatments, metabolic cage experiments were performed to collect urine of these mice. All animal experimental protocols were approved by the Institutional Animal Care and Use Committee of the Virginia Commonwealth University.

2.2. Primary culture of murine podocytes

Primary culture of murine podocytes was performed as described in previous studies [28]. Briefly, we infused 20 mL of dynabeads from the abdominal aorta below the renal artery at

flow rate of 7.4 mL/min/g kidney. After infusion, kidneys were removed, decapsulated, and dissected. The cortex was minced into small pieces and digested with mixture of collagenase A (1 mg/mL) and deoxyribonuclease I (0.2 mg/mL) in Hanks' balanced salt solution at 37 °C for 20 min with gentle agitation. The digested tissue was placed on 100 μM strainer and gently pressed with ice-cold medium. After washing the glomeruli with ice-cold PBS for 6 times, we resuspended the isolated glomeruli with beads into 5 mL medium and transfer them into the collagen I-coated culture flask. After 3 days of culture of isolated glomeruli, cellular outgrowths were detached with Trypsin-ethylenediaminetetraacetic acid solution and transferred to a glass tube. Then, the glass tube was placed onto magnetic particle concentrator for 1 min to remove the glomerular cores and dynabeads. The supernatant was passed through a 40 μm sieve to remove the remaining glomerular cores. The filtered podocytes were cultured in D-MEM/F-12 (1:1) containing 10% fetal bovine serum (Cansera International, Canada) supplemented with 0.5% Insulin–-Transferrin–Selenium-A liquid media supplement (Invitrogen), 100 U/mL penicillin, and 100 mg/mL streptomycin on a new collagen I-coated flask at 37 °C before use in experiments.

2.3. LC-MS/MS analysis

After cell counting, podocytes of WT/WT and Asah1^{fl/fl}/Podo[cre] mice were normalized to 1×10^6 before LC-MS/MS analysis. After homogenization of podocytes, C12 ceramide (10 ng) was added to the homogenate reaction mixture as an internal standard. Then, the mixture was separated in chloroform/methanol/water (2:2:1.8). After evaporation with nitrogen and reconstitution with ethanol/formic acid (99.8:0.2), the samples were ready for LC-MS/MS assay. The separation of ceramide was performed on a Shumadzu SCL HPLC system (Kyoto, Japan) with a C18 Nucleosil AB Column (Macherey-Nagel, Duren, Germany). MS detection was carried out using an Applied Bio systems 3200 Q trap with a turbo V source for TurbolonSpray (Ontario, Canada). The concentrations of total ceramide, including C14, C16, C18, C20, C22, and C24 ceramide, and sphingosine were calculated after normalization with glomerular numbers of each sample. The fragment ion obtained with the highest mass-to-charge ratio (m/z 264) was selected for quantitative MS detection in the multiple reaction monitoring mode.

2.4. GCaMP3 Ca^{2+} imaging

At 18–24 h after nucleofection with GCaMP3-ML1, podocytes were used for experiments [11]. The fluorescence intensity at 470 nm (F470) was recorded with a digital camera (Nikon Diaphoto TMD Inverted Microscope). Metafluor imaging and analysis software were used to acquire, digitize and store the images for offline processing and statistical analysis (Universal Imaging, Bedford Hills, NY, USA). Lysosomal Ca^{2+} release was measured under a 'low' external Ca^{2+} solution, which contained 145 mM NaCl, 5 mM KCl, 3 mM MgCl$_2$, 10 mM glucose, 1 mM EGTA and 20 mM HEPES (pH 7.4). GPN (Cayman Chemical, Ann Arbor, MI, USA) was used as positive control to induce Ca^{2+} release from lysosomes in podocytes. ML-SA1 (Sigma-Aldrich Chemicals, St. Louis, MO, USA) was used as a potent TRPML channel agonist.

2.5. Isolation of lysosomes from podocytes

After treatment with vacuolin-1 (1 μM) for 2 h, isolation of lysosomes was performed [29]. After washing podocytes with pre-cooled PBS, pre-cooled homogenization buffer (0.25 M sucrose, 10 mM Tris, pH = 7.4) was used for detachment of podocytes by a cell scraper. Cell suspension in glass-grinding vessel was homogenized using a Teflon pestle operated at 900 rotations per minute (rpm). The homogenate was then transferred to a 1.5 ml microfuge test tube and centrifuge at 14,000g for 15 min at 4 °C. After centrifuge, the middle part of supernatant was transferred to a 10-ml polycarbonate centrifuge tube. An equal volume of 16 mM CaCl$_2$ was added to precipitate lysosomes. After being shaken on a rotary shaker at 100 rpm for 5 min at 4 °C, supernatant was centrifuged at 25,000g for 15 min at 4 °C in an ultracentrifuge. The supernatant was discarded and the pellet was resuspended in one volume of ice cold washing buffer (150 mM KCl, 10 mM Tris, pH = 7.4). The suspension was centrifuged at 25,000g for 15 min at 4 °C in an ultracentrifuge. After supernatant being discarded, the pellet containing lysosomes was resuspended in 40 μL of washing buffer, which was used for whole-lysosome patch clamp recording. All steps were performed on ice to minimize the activation of damaging from intracellular phospholipases and proteases. Lysosomes were used for electrophysiological recordings within 3 h of isolation to keep lysosomes fresh. To confirm the purity of isolated lysosomes, CytoPainter lysosome staining kit (Abcam, Cambridge, United Kingdom) was used to stain the lysosomes in podocytes before lysosome isolation. The dye working solution was added to the culture medium and incubated at 37 °C for 2 h. After lysosome isolation, the green fluorescence at Ex/Em = 490/525 nm of samples were detected using Guava Easycyte Mini Flow Cytometry System (Guava Technologies, Hayward, CA, USA). The data were analyzed using Guava acquisition and analysis software (Guava Technologies, Hayward, CA, USA).

2.6. Whole-lysosome patch clamp recording

Podocytes were treated with vacuolin-1 (1 μM) for 2 h to increase the size of lysosomes. Using a planar patch clamp system, Port-a-Patch (Nanion Technologies), the whole-lysosome electrophysiology was performed on isolated lysosomes from podocytes [29]. The bath solution contained 60 mM KMSA, 60 mM KF, and 10 mM HEPES (pH 7.2, 2 mM CaMSA was added immediately before starting the measurements to avoid precipitation of CaF2). The luminal solution contained 70 mM KMSA, 60 mM CaMSA, 2 mM MgCl2, and 10 mM HEPES (pH 4.6). The planar patch-clamp technology combined with a pressure control system and microstructured glass chips containing an aperture of around 1 μm diameter (resistances of 10–15 MΩ) (Nanion Technologies). Currents were recorded using an EPC-10 patch-clamp amplifier and PatchMaster acquisition software (HEKA). Data were digitized at 40 kHz and filtered at 2.8 kHz. The membrane potential was held at −60 mV, and 500 ms voltage ramps from −200 to +100 mV were applied every 5 s. All recordings were obtained at room temperature (21–23 °C), and all recordings were analyzed using PatchMaster (HEKA) and Origin 6.1 (OriginLab). The salt-agar bridges were used to connect the reference Ag/AgCl wire to the bath solution to minimize voltage offsets. Ag/AgCl-coated electrodes were chloridated in bleach solution approximately 15 min until a black AgCl-layer was obvious on the silver wire. The liquid junction potential was corrected.

2.7. Confocal microscopy

Double-immunofluorescence staining was performed using cultured podocytes grown on collagen-coated glass coverslips [30,31]. Briefly, after fixation, the cells were incubated with rabbit anti-VPS16 (1:200; proteintech, Rosemont, IL, USA) and rat anti-Lamp-1 (1:200; Abcam Biotechnology, Cambridge, United Kingdom) overnight at 4 °C. Then, Alexa 488-labeled anti-rabbit secondary antibody (1:200; Life Technologies, CA, USA) and Alexa 594-labeled anti-rat secondary antibody (1:200; Life Technologies, CA, USA) were added to the cell slides and incubated for 1 h at room temperature. Slides were then washed, mounted, and observed using a confocal laser scanning microscope (Fluoview FV1000, Olympus, Japan). Sequential laser excitation at 488 and 568 nm and emission collection between 495 and 530 nm and 590–680 nm for fluorescein/EGFP/Alexa Fluor 488 and Alexa Fluor 594, respectively, were used to minimize bleedthrough between the two fluorophores. The zero offset was set with the laser turned off and the photomultiplier gain was adjusted to keep the intensity range, from background to the most intense, within the eight bit digital output range. Podocytes selected for imaging met the criteria of having no nearby podocytes and clearly discernible nuclei with phase contrast. Imaging was performed at the equatorial plane of podocytes. The images were acquired blindly to minimize operator bias. Image Pro Plus 6.0 software (Media Cybernetics, Bethesda, MD, USA) was employed to analyze colocalization, expressed as the Pearson correlation coefficient.

2.8. Nanoparticle tracking analysis

Nanoparticle tracking analysis (NTA) measurements were performed with a NanoSight NTA3.2 Dev Build 3.2.16 (Malvern Instruments Ltd., UK), equipped with a sample chamber with a 638-nm laser and a Viton fluoroelastomer O-ring. The samples were injected in the sample chamber with sterile syringes (BD, New Jersey, USA) until the liquid reached the tip of the nozzle. All measurements were performed at room temperature. The screen gain and camera level were 10 and 13, respectively. Each sample was measured at standard measurement, 30 s with manual shutter and gain adjustments. Three measurements of each sample were performed. 3D figures were exported from the software. Particles sized between 50 and 100 nm were calculated [11].

2.9. Statistical analysis

All of the values are expressed as mean ± SEM. Significant differences among multiple groups were examined using t-test or ANOVA followed by a Student-Newman-Keuls test. $P < 0.05$ was considered statistically significant.

3. Results

3.1. Elevated urinary exosome excretion in mice with podocyte-specific Asah1 gene knockout

By nanoparticle tracking analysis (NTA), we first measured urinary exosome excretion of WT/WT and Asah1^{fl/fl}/Podo[cre] mice. In Fig. 1A, the representative 3-D histograms of urinary exosomes showed that the urinary exosome concentrations remained relatively low in WT/WT mice. However, urinary exosome concentration of Asah1^{fl/fl}/Podo[cre] mice was

obviously higher than WT/WT mice. Summarized data demonstrated that podocyte-specific Asah1 gene knockout remarkably enhanced urinary excretion of exosomes in Asah1$^{fl/fl}$/Podo^{cre} mice. Furthermore, we used immunohistochemical analysis to determine the glomerular level of Annexin-II, an exosome marker, in glomeruli of these mice. Consistent with NTA results, Annexin-II was detected at a low level within glomeruli in WT/WT mice. On the contrary, Asah1 gene deletion in podocytes significantly elevated the glomerular Annexin-II level in Asah1$^{fl/fl}$/Podo^{cre} mice (Fig. 1B).

3.2. Characterization of podocytes isolated from Asah1$^{fl/fl}$/Podo^{cre} mice and their littermates

To further determine the derivation of increased urinary vesicles in Asah1$^{fl/fl}$/Podo^{cre} mice, we isolated and cultured podocytes from WT/WT and Asah1$^{fl/fl}$/Podo^{cre} mice as previously described [28]. As illustrated in Fig. 2A, podocytes isolated from WT/WT mice abundantly expressed podocyte markers such as podocin, nephrin, and synaptopodin, suggesting the normal function of these cells after isolation and primary culture. We next detected the expression of α subunit of Ac in podocytes of different mice by confocal microscopy. The representative images showed that α subunit of Ac was undetectable in podocytes of Asah1$^{fl/fl}$/Podo^{cre} mice (Fig. 2B). Using Western blot analysis, Asah1 gene knockout in podocytes of Asah1$^{fl/fl}$/Podo^{cre} mice was further confirmed (Fig. 2C). Furthermore, we performed LC-MS/MS to determine the levels of Ac-associated sphingolipids in podocytes of WT/WT and Asah1$^{fl/fl}$/Podo^{cre} mice. Total ceramide levels and C16 ceramide, the main substrate of Ac, were analyzed after normalization for the number of cells collected for the analysis. It was found that both total ceramide and C16 ceramide levels were much higher in podocytes of Asah1$^{fl/fl}$/Podo^{cre} mice compared with WT/WT mice. On the other hand, there was no significant difference in the sphingosine level in podocytes of WT/WT and Asah1$^{fl/fl}$/Podo^{Cre} mice (Fig. 2D).

3.3. Enhanced exosome release due to decreased lysosome-MVB interaction

Consistent with in vivo results, the representative 3-D histograms illustrated that WT/WT podocytes released exosomes in a low level after culture for 24 h. Podocytes isolated from Asah1$^{fl/fl}$/Podo^{cre} mice, however, secreted large number of exosomes compared with podocytes of WT/WT mice (Fig. 3A). The summarized data showed that Asah1 gene knockout dramatically enhanced exosome secretion from podocytes. To determine the role of lysosomes in the regulation of exosome release, confocal microscopy was performed to detect lysosome-MVB interaction in these cells. In WT/WT podocytes, we observed considerable colocalization of VPS16 as MVB marker (green fluorescence) and Lamp-1 as lysosome marker (red fluorescence), as shown by yellow spots in these cells. On the contrary, very few colocalization of VPS16 and Lamp-1 was seen in podocytes with Asah1 gene knockout (Fig. 3B). The summarized data confirmed that colocalization of VPS16 and Lamp-1 was significantly reduced by Asah1 gene deletion in podocytes.

3.4. Inhibition of podocyte TRPML1 channel activity by Asah1 gene knockout

Given that lysosomal TRPML1 channel-mediated Ca^{2+} release has been reported to be essential for lysosome trafficking, we tested whether lysosomal TRPML1 channel activity can be altered by Asah1 gene knockout in podocytes. To specifically detect Ca^{2+} release

through lysosomal TRPML1 channel, nucleofection of GCaMP3-ML1 plasmid into podocytes was performed to express GCaMP3, a single-wavelength genetically encoded Ca^{2+} indicator, on the cytoplasmic amino terminus of TRPML1 in these cells as described in our previous studies [11]. A fluorescent microscopic imaging system was used to dynamically and continuously monitor the GCaMP3 fluorescence signal (F470) in podocytes. The intensity of Ca^{2+}-induced GCaMP3 fluorescence indicated the amount of Ca^{2+} released through lysosomal TRPML1 channel. As shown in Fig. 4A and B, the GCaMP3 fluorescence detected in WT/WT podocytes was weak under control condition. ML-SA1 as a TRPML1 channel agonist induced a rapid elevation of GCaMP3 fluorescence in these cells, which was followed by a large signal increase caused by late addition of ionomycin, a Ca^{2+} ionophore. In contrast, ML-SA1 failed to augment GCaMP3 fluorescence in podocytes of Asah1$^{fl/fl}$/Podo^{cre} mice, while ionomycin still stimulated a dramatic elevation of GCaMP3 fluorescence in these cells. The summarized data showed that ML-SA1 induced remarkable TRPML1 channel-mediated Ca^{2+} release in podocytes which was almost blocked by Asah1 gene knockout (Fig. 4C). Western blot analysis was performed to test whether Asah1 gene deletion changed TRPML1 channel expression in podocytes. It was found that expression of TRPML1 channel in podocytes was not affected by Asah1 gene deletion (Supplementary Fig. 1). Next, we examined the effect of sphingosine (Sph) as the product of ceramide metabolism by Ac on the opening of TRPML1 channel. By GCaMP3 Ca^{2+} imaging, Sph was demonstrated to induce lysosomal Ca2+ release through TRPML1 channel in WT/WT podocytes in a dose-dependent manner (Supplementary Fig. 2). Interestingly, Sph induced substantial Ca^{2+} release through TRPML1 channel in podocytes of WT/WT mice as well as Asah1$^{fl/fl}$/Podo^{cre} mice (Fig. 5). Given that Sph can be phosphorylated to sphingosine-1-phosphate (S1P), an important signal molecule, we tested whether S1P regulates TRPML1 channel. It was found that S1P had no effects on TRPML1 channel activity (Supplementary Fig. 3).

3.5. Role of different sphingolipids in regulation of TRPML1 channel activity

To further dissect the actions of Ac-associated sphingolipids on TRPML1 channel activity, lysosomes of these cells were isolated from podocytes of WT/WT and Asah1$^{fl/fl}$/Podo^{cre} mice for whole-lysosome patch clamping. After treatment with vacuolin-1, podocytes were enlarged and then isolated for experiments as described in our previous studies [11]. To characterize the function of TRPML1 channel in isolated lysosomes, we stimulated patched lysosomes with ML-SA1 in 3 different doses in the bath solution. It was found that bath application of ML-SA1 induced Ca^{2+} release from lysosome of WT/WT podocytes in a dose-dependent manner (Fig. 6A and B). However, there was no significant increase observed in lysosomal Ca^{2+} currents after addition of ML-SA1 into bath solution (Fig. 6C). Next, we measured lysosomal Ca^{2+} release in response to Ac-associated sphingolipids such as sphingomyelin (SM), C16 ceramide (Cer), and sphingosine (Sph) to determine their regulatory role on TRPML1 channel. As illustrated in Fig. 6D, SM, Cer, and Sph had different effects on Ca^{2+} release of lysosomes isolated from WT/WT podocytes, with inhibition by SM, no effect by Cer, but enhancement by Sph. Although both SM and Cer produced no effect on Ca^{2+} release of lysosomes isolated from podocytes with Asah1 gene knockout, Sph remained to increase TRPML1 channel activity in these lysosomes (Fig. 6E).

3.6. Inhibition of exosome release by enhancement of TRPML1 channel activity

Based on our findings, enhancement of TRPML1 channel activity may be a potential therapeutic strategy against elevated exosome secretion from podocytes in Asah1$^{fl/fl}$/Podo^{cre} mice. To test this hypothesis, we treated podocytes of WT/WT and Asah1$^{fl/fl}$/Podo^{cre} mice with C2 ceramide (Cer) or Sph for 24 h before further experiments. In Fig. 7A, the representative 3-D histograms of vesicles showed that podocytes of Asah1$^{fl/fl}$/Podo^{cre} mice released much less exosomes after treatment with Sph but not Cer. The summarized data of NTA demonstrated that exosomes released from podocytes lacking Asah1 gene were significantly decreased after treatment with Sph. Also, confocal microscopy was performed to detect lysosome-MVB interaction in these cells after treatments. As shown in Fig. 7B, obvious increase in colocalization of VPS16 and Lamp-1 indicated by yellow spots was found in podocytes of WT/WT mice as well as Asah1$^{fl/fl}$/Podo^{cre} mice after treatment with Sph compared with vehicle and Cer groups. The summarized data showed that colocalization of VPS16 and Lamp-1 in podocytes of both groups of mice was significantly increased by Sph. Moreover, we tested whether sphingosine inhibited urinary exosome excretion in Asah1$^{fl/fl}$/Podo^{cre} mice. WT/WT and Asah1$^{fl/fl}$/Podo^{cre} mice at 8 weeks were treated with vehicle, *N, N*-dimethylsphingosine (DMS), or combination of DMS and Sph daily for 2 weeks. After treatment, the urine samples of these mice were collected and NTA was performed to determine the level of urinary exosome excretion of these mice. As shown in Fig. 8, no significant changes of urinary exosome excretion were found between vehicle-treated mice and DMS-treated mice. The combination of DMS and Sph, however, significantly decreased urinary exosome excretion of both WT/WT and Asah1$^{fl/fl}$/Podo^{cre} mice.

3.7. Downregulation of exosome release by overexpression of Asah1 gene

To further confirm the role of Ac activity in the regulation of ceramide metabolism and exosome release from podocytes, we used a podocyte-specific full-length Ac gene expression vector (GeneCopoeia, Cat#: MPRM47536-PF02) to overexpress Asah1 gene in WT/WT podocytes or rescue Asah1 gene in podocytes of Asah1$^{fl/fl}$/Podo^{cre} mice. By immunofluorescent staining, we demonstrated that overexpression of Asah1 gene in podocytes significantly upregulated the level of Ac expression in WT/WT podocytes but failed to affect ceramide level in these cells. Podocyte-specific full-length Ac gene expression vector rescued the expression of Ac and totally blocked ceramide accumulation in podocytes of Asah1$^{fl/fl}$/Podo^{cre} mice (Fig. 9A). As shown in Fig. 9B, NTA results showed that overexpression of Asah1 gene obviously reduced exosome secretion from WT/WT podocytes. Recovery of Ac expression was found to prevent the increase in exosome release from podocytes of Asah1$^{fl/fl}$/Podo^{cre} mice. As a control plasmid, mock vector produced no effects on both types of cells.

4. Discussion

The major goal of the present study was to determine whether podocyte exosome secretion is enhanced by Asah1 gene knockout via inhibition of TRPML1 channel activity, which may serve as a pathogenic mechanism of podocytopathy and NS in Asah1$^{fl/fl}$/Podo^{Cre} mice. Our results demonstrated a remarkable enhancement of exosome release from podocytes in vivo

and in vitro in Asah1$^{fl/fl}$/Podo^{Cre} mice, which was attributed to reduced degradation of MVBs by lysosomes in these cells. Treatment with Ac product, Sph completely blocked exosome secretion by recovering the lysosome-MVB interaction in podocytes of Asah1$^{fl/fl}$/Podo^{Cre} mice. These results suggest that Asah1 gene expression critically contributes to the control of lysosome TRPML1 channel activity and consequently regulates the interaction of lysosome-MVB interaction determining exosome release.

Recent studies in our laboratory have demonstrated that podocytopathy and steroid-resistant NS occur in mice with podocyte-specific Asah1 gene deletion [21]. However, the pathogenesis of podocytopathy and NS in these mice remains unclear. In this regard, there is evidence that urinary exosomes not only indicate the physiological or pathological condition of kidney as a biomarker, but also participate in the initiation or development of various kidney diseases [15-17]. More specifically, many reports have shown that podocyte-derived exosomes increased in accompany with albuminuria and glomerular degeneration in patients with FSGS and NS [15,23]. Furthermore, podocyte-derived exosomes have been reported to be detectable in urine even before the onset of albuminuria in diabetic mice [18]. Given that exosome biogenesis and secretion have been reported to be critically regulated by ceramide signaling pathway in different tissues and cells [32], the present study tested whether podocyte-specific Asah1 gene deletion leads to ceramide increase in podocyte and thereby augments exosome release from these cells. By NTA, it was found that urinary exosome excretion in Asah1$^{fl/fl}$/Podo^{cre} mice was remarkably enhanced. IHC detection demonstrated that exosomes were significantly accumulated in glomeruli. Consistent with these in vivo results, exosomes were also found to be abundantly released from isolated and cultured podocytes with Asah1 gene deletion. Together, these results suggest that Asah1$^{fl/fl}$/Podo^{cre} mice with podocytopathy have enhanced podocyte-derived exosomes release and their enrichment in glomeruli. To our knowledge, our findings support the view that Asah1 gene expression is indeed implicated in the control of exosome release from podocytes.

Another interesting finding of the present study is that the lysosome-MVB interaction was obviously inhibited in podocytes isolated from Asah1$^{fl/fl}$/Podo^{cre} mice. These results imply that lysosome may determine the MVB fate in podocytes, which may be a major mechanism to result in robust exosome release from podocytes lacking Asah1 gene. Our results are consistent with previous studies reporting that lysosomes are essential for the degradation of MVBs and autophagosomes in podocytes [11,19,33,34]. In other types of cells such as neurons, epithelial cells, and vascular cells, increased exosome release was found after inhibition of lysosome function [6-8]. In addition, MVBs were found to fuse with autophagosomes to form amphisomes and subsequently fuse with lysosomes to terminate MVB fate and thereby reduce exosome release [35,36]. Our results support the view that augmented exosome release may be attributed to reduced lysosome-MVB interaction in podocytes with Asah1 gene knockout.

The present study determined how Asah1 gene deletion attenuates the lysosome-MVB interaction and increased exosome secretion in podocytes. It has been reported that the trafficking of lysosomes is essential for the fusion of lysosomes and MVBs, which depends on lysosomal Ca^{2+} release [9-11]. In this regard, it is well known that lysosomal Ca^{2+} is released through TRPML1 channel in response to endogenously produced NAADP [37-40]

or other factors like PIPs (PI (3,5)P2) and irons [9,41]. Recently, lysosomal TRPML1 channel activity has been shown to be regulated by sphingolipids, which serve as a key mechanism determining lysosome trafficking, where accumulated SM inhibited its activity and reduced lysosomal Ca^{2+} release, leading to failure of lysosome trafficking and lysosomal storage disease, as shown in Niemann-Pick disease [10]. Sph, a Cer metabolite via Ac was also found to activate TRPML1 channels, promoting lysosome Ca^{2+} release and trafficking. We recently reported that lysosomal TRPML1 channel-mediated Ca^{2+} release is controlled by Ac [11]. Based on these observations, we hypothesized that Asah1 gene deletion and associated changes in sphingolipids block TRPML1 channel-mediated Ca^{2+} release from lysosomes and thereby inhibit a Ca^{2+}-dependent lysosome trafficking in podocytes of Asah1$^{fl/fl}$/Podo^{cre} mice. By GCaMP3 Ca^{2+} imaging and whole lysosome patch clamping, we indeed confirmed that TRPML1 channel agonist ML-SA1 induced remarkable and rapid lysosomal Ca^{2+} release in podocyte of WT/WT mice. Coinciding with deficient lysosome trafficking, Asah1 gene knockout resulted in failure of ML-SA1 to induce TRPML1 channel-mediated Ca^{2+} release in podocytes. Sph as the product of Ac, however, rescued the function of TRPML1 channel in podocytes lacking Asah1 gene. Functionally, treatment of podocytes from Asah1$^{fl/fl}$/Podo^{Cre} mice with sphingosine was found to recover lysosome-MVB interaction and reduce exosome release. Correspondingly, the combination of DMS and Sph remarkably inhibited urinary exosome excretion of Asah1$^{fl/fl}$/Podo^{Cre} mice. Furthermore, we demonstrated that rescue of Asah1 gene obviously decreased exosome release from podocytes of Asah1$^{fl/fl}$/Podo^{Cre} mice. These results suggest that dysregulation of TRPML1 channel activity and consequent increase in exosome release are attributed to the reduction of Sph in podocytes with Asah1 gene deletion. To our knowledge, these results provide the first experimental evidence that normal Asah1 gene expression is essential for the control of TRPML1 channel activity via Sph and that Asah1 gene knockout will lead to dysregulation of this channel and result in increased exosome secretion from podocytes. In this regard, our previous studies have shown that hyperhomocysteinemia (hHcy) induces ASM overexpression and thereby results in renal Cer accumulation, podocyte injury, and glomerular sclerosis [22,42]. Obesity-induced NLRP3 inflammasome activation in podocytes and glomerular injury are attributed to the overexpression of ASM [43]. The deficiency of Smpd1 gene, however, prevents podocyte injury and glomerular sclerosis during hHcy and obesity [22,42,43]. Moreover, inhibition of ASM activity has recently been reported to attenuate D-ribose-induced Cer accumulation and abundant exosome release in podocytes [19]. In patients with diabetic kidney disease, the mRNA expression of acid sphingomyelinase-like phosphodiesterase 3b (SMPDL3b) in glomeruli is significantly increased compared with controls. Furthermore, knockout of SMPDL3b protects podocytes from apoptosis induced by soluble urokinase plasminogen activator receptor (suPAR) [44]. On the contrary, it has been reported that the expression of SMPDL3b is decreased in podocytes in patients with recurrent FSGS. The disruption of actin cytoskeleton and podocyte apoptosis induced by patient sera are blocked by overexpression of SMPDL3b [45]. These results suggest that both accumulation and reduction in Cer due to imbalance of associated enzyme activity may result in podocyte injury and renal diseases through different mechanisms. Our findings together with these previous studies provide strong evidence that Cer metabolism by Ac may play an important role in the maintenance of podocyte integrity and function. Disruption of Cer metabolism

Author Manuscript

Author Manuscript

Author Manuscript

Author Manuscript

and Sph production by Ac may alter lysosome function and exosome release, which is a potential pathological mechanism of podocyte injury and nephrotic syndrome.

In summary, the present study demonstrated in in vivo and in vitro experiments that Asah1 gene knockout inhibited TRPML1 channel activity via alteration of sphingolipid metabolism to reduce Sph, which caused less lysosome-MVB interaction and more exosome secretion in podocytes. Sph was shown to rescue the lysosome-MVB interaction and attenuate exosome release. It is concluded that Sph from Cer via Ac importantly controls TRPML1 channel activity and determine the MVB fate and exosome release. Given that podocyte-specific Asah1 gene knockout has been reported to induce podocytopathy, our findings indicate that podocyte-derived exosomes may initiate or enhance podocyte injury in Asah1$^{fl/fl}$/Podo^{cre} mice duo to the dysregulation of TRPML1 channel activity and the reduced lysosome-MVB interaction. Targeting TRPML1 channel may be a potential therapeutic strategy to attenuate podocyte-derived exosome release and consequent podocytopathy under pathological conditions.

Supplementary Material

Refer to Web version on PubMed Central for supplementary material.

Acknowledgments

Abbreviations

|	
NS	nephrotic syndrome
Ac	acid ceramidase
MVB	multivesicular body
TRPML1	transient receptor potential mucolipin 1
EV	extracellular vesicle
FSGS	focal segmental glomerular sclerosis
NTA	nanoparticle tracking analysis
Sph	sphingosine
SM	sphingomyelin
Cer	ceramide
S1P	sphingosine-1-phosphate
DMS, N	*N*-dimethylsphingosine

References

[1]. Crescitelli R, Lasser C, Szabo TG, Kittel A, Eldh M, Dianzani I, Buzas EI, Lotvall J, Distinct RNA profiles in subpopulations of extracellular vesicles: apoptotic bodies, microvesicles and exosomes, J. Extracell. Vesicles 2 (2013).

[2]. Lazaro-Ibanez E, Sanz-Garcia A, Visakorpi T, Escobedo-Lucea C, Siljander P, Ayuso-Sacido A, Yliperttula M, Different gDNA content in the subpopulations of prostate cancer extracellular vesicles: apoptotic bodies, microvesicles, and exosomes, Prostate 74 (2014) 1379–1390. [PubMed: 25111183]

[3]. Rajagopal C, Harikumar KB, The origin and functions of exosomes in cancer, Front. Oncol 8 (2018) 66. [PubMed: 29616188]

[4]. Futter CE, Pearse A, Hewlett LJ, Hopkins CR, Multivesicular endosomes containing internalized EGF-EGF receptor complexes mature and then fuse directly with lysosomes, J. Cell Biol 132 (1996) 1011–1023. [PubMed: 8601581]

[5]. Hessvik NP, Llorente A, Current knowledge on exosome biogenesis and release, Cell. Mol. Life Sci. CMLS 75 (2018) 193–208. [PubMed: 28733901]

[6]. Alvarez-Erviti L, Seow Y, Schapira AH, Gardiner C, Sargent IL, Wood MJ, Cooper JM, Lysosomal dysfunction increases exosome-mediated alpha-synuclein release and transmission, Neurobiol. Dis 42 (2011) 360–367. [PubMed: 21303699]

[7]. Vingtdeux V, Hamdane M, Loyens A, Gele P, Drobeck H, Begard S, Galas MC, Delacourte A, Beauvillain JC, Buee L, Sergeant N, Alkalizing drugs induce accumulation of amyloid precursor protein by-products in luminal vesicles of multivesicular bodies, J. Biol. Chem 282 (2007) 18197–18205. [PubMed: 17468104]

[8]. Miranda AM, Lasiecka ZM, Xu Y, Neufeld J, Shahriar S, Simoes S, Chan RB, Oliveira TG, Small SA, Di Paolo G, Neuronal lysosomal dysfunction releases exosomes harboring APP C-terminal fragments and unique lipid signatures, Nat. Commun 9 (2018) 291. [PubMed: 29348617]

[9]. Dong XP, Shen D, Wang X, Dawson T, Li X, Zhang Q, Cheng X, Zhang Y, Weisman LS, Delling M, Xu H, PI(3,5)P(2) controls membrane trafficking by direct activation of mucolipin Ca(2+) release channels in the endolysosome, Nat. Commun 1 (2010) 38. [PubMed: 20802798]

[10]. Shen D, Wang X, Li X, Zhang X, Yao Z, Dibble S, Dong XP, Yu T, Lieberman AP, Showalter HD, Xu H, Lipid storage disorders block lysosomal trafficking by inhibiting a TRP channel and lysosomal calcium release, Nat. Commun 3 (2012) 731. [PubMed: 22415822]

[11]. Li G, Huang D, Hong J, Bhat OM, Yuan X, Li PL, Control of lysosomal TRPML1 channel activity and exosome release by acid ceramidase in mouse podocytes, Am. J. Physiol. Cell Physiol 317 (2019) C481–C491. [PubMed: 31268777]

[12]. Boulanger CM, Loyer X, Rautou PE, Amabile N, Extracellular vesicles in coronary artery disease, Nat. Rev. Cardiol 14 (2017) 259–272. [PubMed: 28150804]

[13]. Bruno S, Porta S, Bussolati B, Extracellular vesicles in renal tissue damage and regeneration, Eur. J. Pharmacol 790 (2016) 83–91. [PubMed: 27375075]

[14]. Chistiakov DA, Orekhov AN, Bobryshev YV, Extracellular vesicles and atherosclerotic disease, Cell. Mol. Life Sci. CMLS 72 (2015) 2697–2708. [PubMed: 25894694]

[15]. Erdbrugger U, Le TH, Extracellular vesicles in renal diseases: more than novel biomarkers? J. Am. Soc. Nephrol 27 (2016) 12–26. [PubMed: 26251351]

[16]. Street JM, Birkhoff W, Menzies RI, Webb DJ, Bailey MA, Dear JW, Exosomal transmission of functional aquaporin 2 in kidney cortical collecting duct cells, J. Physiol 589 (2011) 6119–6127. [PubMed: 22025668]

[17]. Wu X, Gao Y, Xu L, Dang W, Yan H, Zou D, Zhu Z, Luo L, Tian N, Wang X, Tong Y, Han Z, Exosomes from high glucose-treated glomerular endothelial cells trigger the epithelial-mesenchymal transition and dysfunction of podocytes, Sci. Rep 7 (2017) 9371. [PubMed: 28839221]

[18]. Zhou H, Kajiyama H, Tsuji T, Hu X, Leelahavanichkul A, Vento S, Frank R, Kopp JB, Trachtman H, Star RA, Yuen PS, Urinary exosomal Wilms' tumor-1 as a potential biomarker for podocyte injury, Am. J. Physiol. Renal Physiol 305 (2013) F553–F559. [PubMed: 23761678]

[19]. Hong J, Bhat OM, Li G, Dempsey SK, Zhang Q, Ritter JK, Li W, Li PL, Lysosomal regulation of extracellular vesicle excretion during d-ribose-induced NLRP3 inflammasome activation in podocytes, Biochim. Biophys. Acta Mol. Cell. Res 1866 (2019) 849–860. [PubMed: 30771382]

[20]. Jin J, Wang Y, Zhao L, Zou W, Tan M, He Q, Exosomal miRNA-215-5p derived from adipose-derived stem cells attenuates epithelial-mesenchymal transition of podocytes by inhibiting ZEB2, Biomed. Res. Int 2020 (2020), 2685305. [PubMed: 32149094]

[21]. Li G, Kidd J, Kaspar C, Dempsey S, Bhat OM, Camus S, Ritter JK, Gehr TWB, Gulbins E, Li PL, Podocytopathy and Nephrotic syndrome in mice with podocyte-specific deletion of the Asah1 gene: role of ceramide accumulation in glomeruli, Am. J. Pathol 190 (2020) 1211–1223. [PubMed: 32194052]

[22]. Boini KM, Xia M, Li C, Zhang C, Payne LP, Abais JM, Poklis JL, Hylemon PB, Li PL, Acid sphingomyelinase gene deficiency ameliorates the hyperhomocysteinemia-induced glomerular injury in mice, Am. J. Pathol 179 (2011) 2210–2219. [PubMed: 21893018]

[23]. Lee H, Han KH, Lee SE, Kim SH, Kang HG, Cheong HI, Urinary exosomal WT1 in childhood nephrotic syndrome, Pediatr. Nephrol 27 (2012) 317–320. [PubMed: 22076591]

[24]. Lytvyn Y, Xiao F, Kennedy CR, Perkins BA, Reich HN, Scholey JW, Cherney DZ, Burger D, Assessment of urinary microparticles in normotensive patients with type 1 diabetes, Diabetologia 60 (2017) 581–584. [PubMed: 28004150]

[25]. Stahl AL, Johansson K, Mossberg M, Kahn R, Karpman D, Exosomes and microvesicles in normal physiology, pathophysiology, and renal diseases, Pediatr. Nephrol 34 (2019) 11–30. [PubMed: 29181712]

[26]. Lai WQ, Goh HH, Bao Z, Wong WS, Melendez AJ, Leung BP, The role of sphingosine kinase in a murine model of allergic asthma, J. Immunol 180 (2008) 4323–4329. [PubMed: 18322246]

[27]. Lee TK, Man K, Ho JW, Wang XH, Poon RT, Xu Y, Ng KT, Chu AC, Sun CK, Ng IO, Sun HC, Tang ZY, Xu R, Fan ST, FTY720: a promising agent for treatment of metastatic hepatocellular carcinoma, Clin. Cancer Res. Off. J. Am. Assoc. Cancer Res 11 (2005) 8458–8466.

[28]. Katsuya K, Yaoita E, Yoshida Y, Yamamoto Y, Yamamoto T, An improved method for primary culture of rat podocytes, Kidney Int. 69 (2006) 2101–2106. [PubMed: 16625147]

[29]. Schieder M, Rotzer K, Bruggemann A, Biel M, Wahl-Schott C, Planar patch clamp approach to characterize ionic currents from intact lysosomes, Sci. Signal 3 (2010) (pl3).

[30]. Zhang C, Boini KM, Xia M, Abais JM, Li X, Liu Q, Li PL, Activation of Nod-like receptor protein 3 inflammasomes turns on podocyte injury and glomerular sclerosis in hyperhomocysteinemia, Hypertension 60 (2012) 154–162. [PubMed: 22647887]

[31]. Maciel W, Lopes WD, Cruz B, Teixeira W, Felippelli G, Sakamoto CA, Favero FC, Buzzulini C, Soares V, Gomes LV, Bichuette M, da Costa AJ, Effects of *Haematobia irritans* infestation on weight gain of Nelore calves assessed with different antiparasitic treatment schemes, Prev. Vet. Med 118 (2015) 182–186. [PubMed: 25465474]

[32]. Elsherbini A, Bieberich E, Ceramide and exosomes: a novel target in cancer biology and therapy, Adv. Cancer Res 140 (2018) 121–154. [PubMed: 30060807]

[33]. Xiong J, Xia M, Xu M, Zhang Y, Abais JM, Li G, Riebling CR, Ritter JK, Boini KM, Li PL, Autophagy maturation associated with CD38-mediated regulation of lysosome function in mouse glomerular podocytes, J. Cell. Mol. Med 17 (2013) 1598–1607. [PubMed: 24238063]

[34]. Li G, Li CX, Xia M, Ritter JK, Gehr TW, Boini K, Li PL, Enhanced epithelial-to-mesenchymal transition associated with lysosome dysfunction in podocytes: role of p62/Sequestosome 1 as a signaling hub, Cell. Physiol. Biochem 35 (2015) 1773–1786. [PubMed: 25832774]

[35]. Baixauli F, Lopez-Otin C, Mittelbrunn M, Exosomes and autophagy: coordinated mechanisms for the maintenance of cellular fitness, Front. Immunol 5 (2014) 403. [PubMed: 25191326]

[36]. Fader CM, Sanchez D, Furlan M, Colombo MI, Induction of autophagy promotes fusion of multivesicular bodies with autophagic vacuoles in k562 cells, Traffic 9 (2008) 230–250. [PubMed: 17999726]

[37]. Zhang F, Li PL, Reconstitution and characterization of a nicotinic acid adenine dinucleotide phosphate (NAADP)-sensitive Ca2+ release channel from liver lysosomes of rats, J. Biol. Chem 282 (2007) 25259–25269. [PubMed: 17613490]

[38]. Zhang F, Xia M, Li PL, Lysosome-dependent Ca(2+) release response to Fas activation in coronary arterial myocytes through NAADP: evidence from CD38 gene knockouts, Am. J. Physiol. Cell. Physiol 298 (2010) C1209–C1216. [PubMed: 20200208]

[39]. Zhang F, Xu M, Han WQ, Li PL, Reconstitution of lysosomal NAADP-TRP-ML1 signaling pathway and its function in TRP-ML1(−/−) cells, Am. J. Physiol. Cell Physiol 301 (2011) C421–C430. [PubMed: 21613607]

[40]. Zhang F, Zhang G, Zhang AY, Koeberl MJ, Wallander E, Li PL, Production of NAADP and its role in Ca2+ mobilization associated with lysosomes in coronary arterial myocytes, Am. J. Physiol. Heart Circ. Physiol 291 (2006) H274–H282. [PubMed: 16473958]

[41]. Dong XP, Cheng X, Mills E, Delling M, Wang F, Kurz T, Xu H, The type IV mucolipidosis-associated protein TRPML1 is an endolysosomal iron release channel, Nature 455 (2008) 992–996. [PubMed: 18794901]

[42]. Boini KM, Xia M, Abais JM, Xu M, Li CX, Li PL, Acid sphingomyelinase gene knockout ameliorates hyperhomocysteinemic glomerular injury in mice lacking cystathionine-beta-synthase, PLoS One 7 (2012), e45020. [PubMed: 23024785]

[43]. Boini KM, Xia M, Koka S, Gehr TW, Li PL, Instigation of NLRP3 inflammasome activation and glomerular injury in mice on the high fat diet: role of acid sphingomyelinase gene, Oncotarget 7 (2016) 19031–19044. [PubMed: 26980705]

[44]. Yoo TH, Pedigo CE, Guzman J, Correa-Medina M, Wei C, Villarreal R, Mitrofanova A, Leclercq F, Faul C, Li J, Kretzler M, Nelson RG, Lehto M, Forsblom C, Groop PH, Reiser J, Burke GW, Fornoni A, Merscher S, Sphingomyelinase-like phosphodiesterase 3b expression levels determine podocyte injury phenotypes in glomerular disease, J. Am. Soc. Nephrol 26 (2015) 133–147. [PubMed: 24925721]

[45]. Fornoni A, Sageshima J, Wei C, Merscher-Gomez S, Aguillon-Prada R, Jauregui AN, Li J, Mattiazzi A, Ciancio G, Chen L, Zilleruelo G, Abitbol C, Chandar J, Seeherunvong W, Ricordi C, Ikehata M, Rastaldi MP, Reiser J, Burke GW 3rd, Rituximab targets podocytes in recurrent focal segmental glomerulosclerosis, Sci. Transl. Med 3 (2011), 85ra46.

A

WT/WT   Asah1$^{fl/fl}$/Podo^{cre}

B

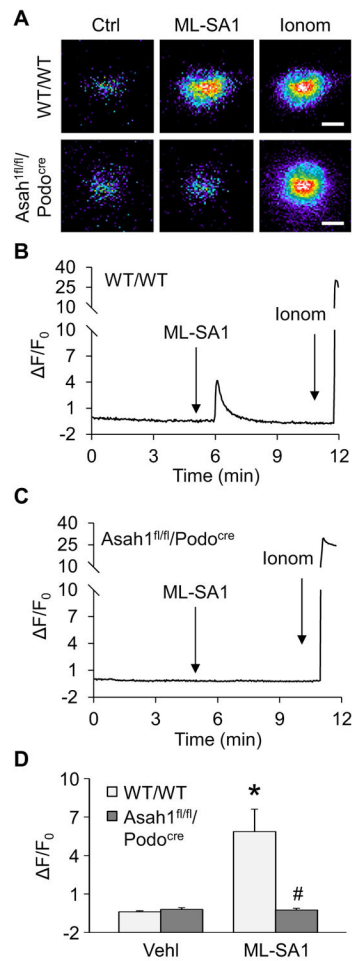WT/WT   Asah1$^{fl/fl}$/Podo^{cre}
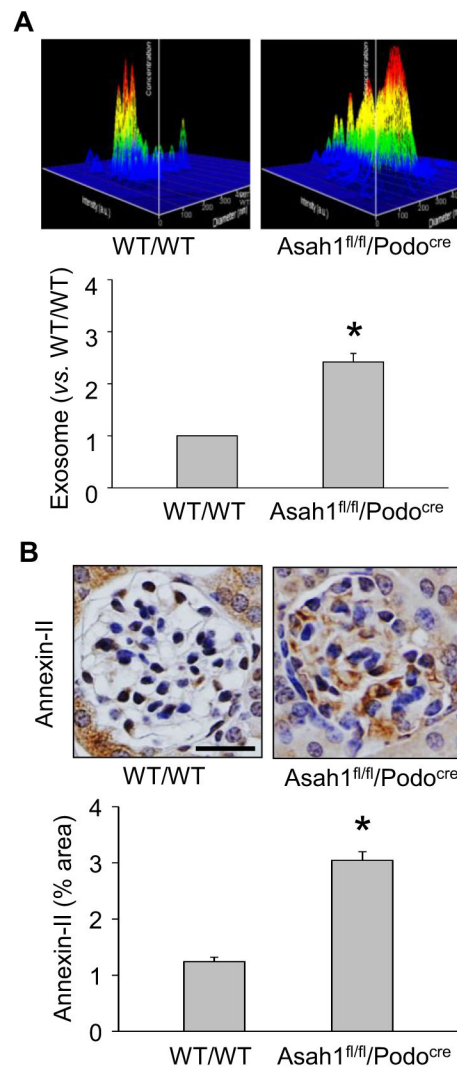
Fig. 1.
Elevated urinary exosome excretion in mice with podocyte-specific Asah1 gene knockout.
A. Representative images and summarized data showing that podocyte-specific Asah1 gene knockout remarkably enhanced urinary exosome excretion ($n = 6$). B. Representative images and summarized data showing that glomerular Annexin-II was significantly higher in Asah1$^{fl/fl}$/Podo^{cre} mice compared with WT/WT mice (n = 6). Scale bars = 50 μm. *$p < 0.05$ vs. WT/WT group.
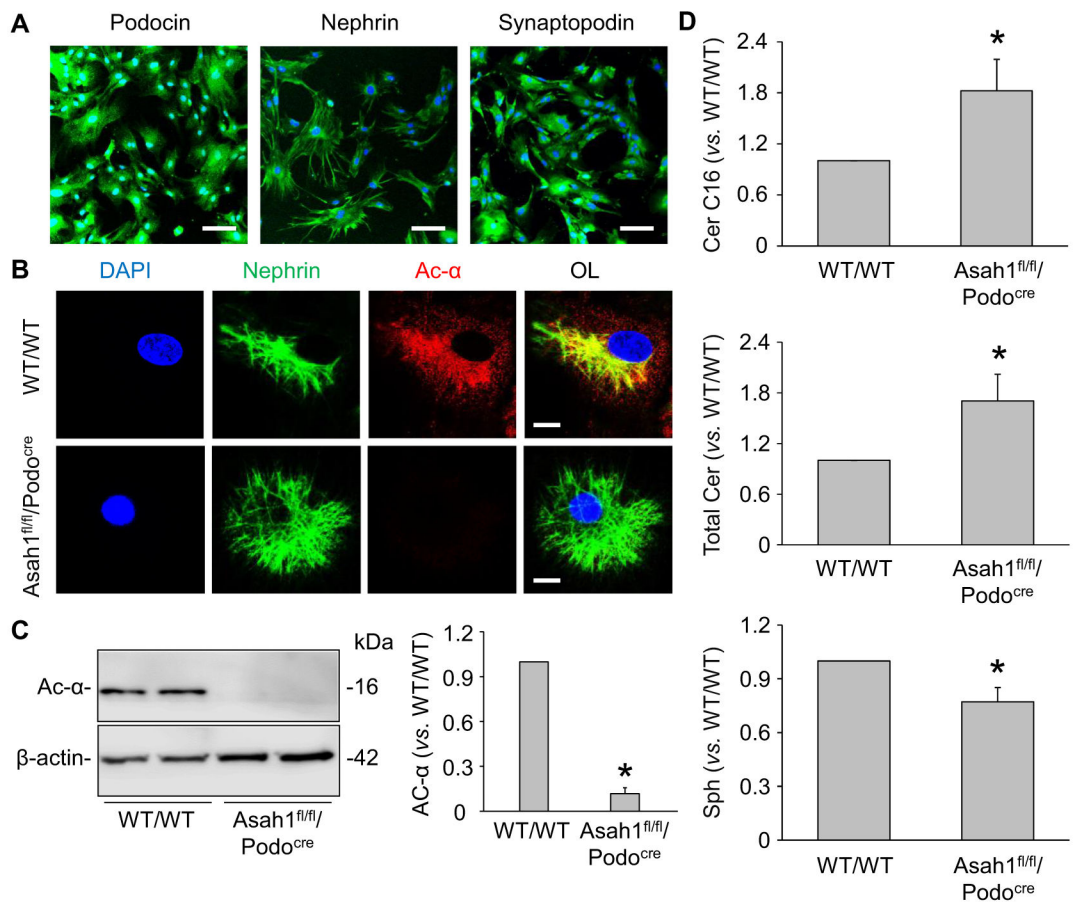
Fig. 2.
Characterization of podocytes isolated from Asah1$^{fl/fl}$/Podo^{cre} mice and their littermates. A. Representative images showing the immunofluorescent staining of podocin, nephrin, and synaptopodin in podocytes isolated from WT/WT mice ($n = 4$). Scale bars = 100 μm. B. Representative images showing that Ac was undetectable in podocytes isolated from Asah1$^{fl/fl}$/Podo^{cre} mice (n = 4). Scale bars = 20 μm. C. Representative gel documents and summarized data showing that Ac was not expressed in podocytes isolated from Asah1$^{fl/fl}$/Podo^{cre} mice ($n = 6$). D. Summarized data showing the levels of C16 ceramide, total ceramide, and sphingosine in podocytes isolated from WT/WT and Asah1$^{fl/fl}$/Podo^{cre} mice (n = 5–6). $*p < 0.05$ vs. WT/WT group.
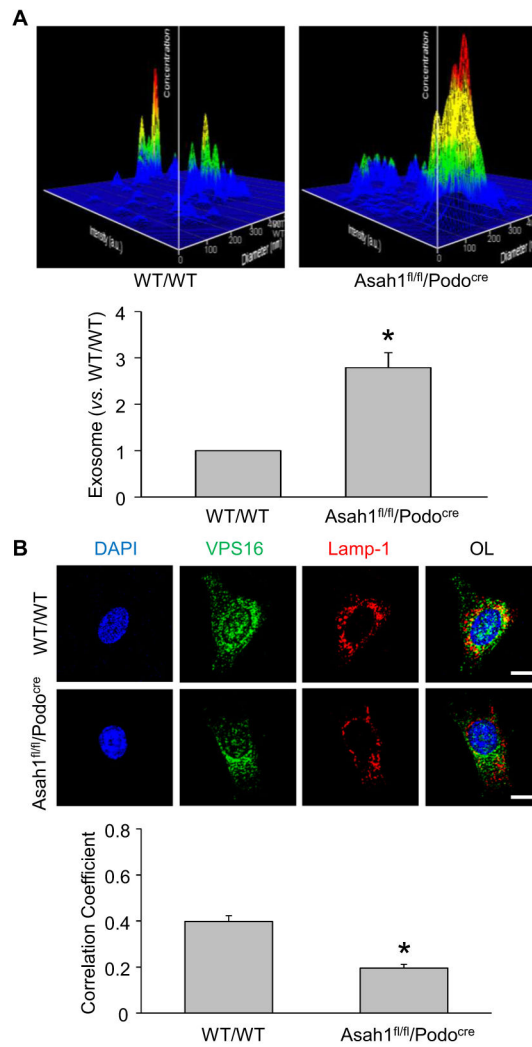
Fig. 3.
Enhanced exosome release due to decreased lysosome-MVB interaction. A. Representative images and summarized data showing that exosome release were remarkably elevated in podocytes isolated from Asah1$^{fl/fl}$/Podo^{cre} mice (n = 6). B. Representative images and summarized data showing that lysosome-MVB interaction was significantly attenuated in podocytes lacking Asah1 gene ($n = 9$). Scale bars = 20 μm. $*p < 0.05$ vs. WT/WT group.

Fig. 4.
Failure of ML-SA1 to induce Ca^{2+} release through TRPML1 channel in podocytes lacking Asah1 gene. A. Representative images showing that ML-SA1 (20 μM) induced TRPML1 channel-mediated Ca^{2+} release in podocytes of WT/WT mice but not Asah1$^{fl/fl}$/Podo^{cre} mice. Scale bars = 40 μm. B. A representative curve showing that ML-SA1 induced elevation of GCaMP3 signal in podocytes of WT/WT mice. C. A representative curve showing that ML-SA1 did not induce elevation of GCaMP3 signal in podocytes of Asah1$^{fl/fl}$/Podo^{cre} mice. D. Summarized data showing that Asah1 gene knockout blocked TRPML1-mediated Ca^{2+} release induced by ML-SA1 in podocytes ($n = 4$–5). *$p < 0.05$ vs. Vehl group, $^{\#}p < 0.05$ vs. WT/WT group. Ctrl, control; Ionom, ionomycin; Vehl, vehicle.
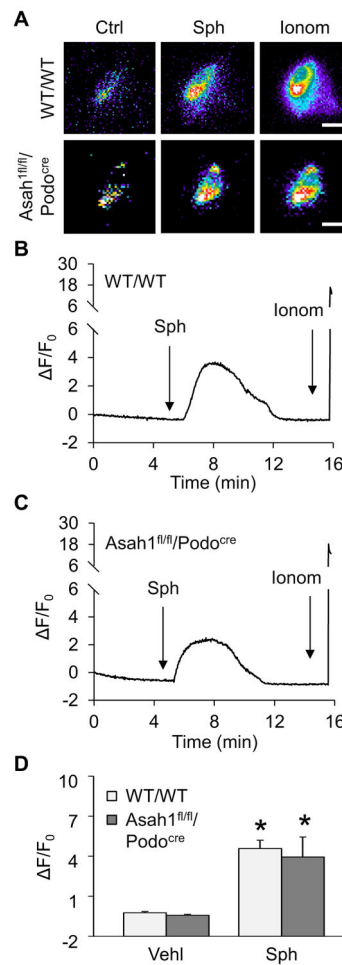
Fig. 5.

Rescue of TRPML1 channel function by Sph in podocytes with Asah1 gene deletion. A. Representative images showing that Sph (20 μM) induced TRPML1 channel-mediated Ca^{2+} release in podocytes of both WT/WT and Asah1$^{fl/fl}$/Podo^{cre} mice. Scale bars = 40 μm. B. A representative curve showing that Sph induced elevation of GCaMP3 signal in podocytes of WT/WT mice. C. A representative curve showing that Sph induced elevation of GCaMP3 signal in podocytes of Asah1$^{fl/fl}$/Podo^{cre} mice. D. Summarized data showing that Sph rescued TRPML1 channel function in podocytes lacking Asah1 gene (n = 4–5). *p < 0.05 vs. Vehl group. Ctrl, control; Sph, sphingosine; Ionom, ionomycin; Vehl, vehicle.
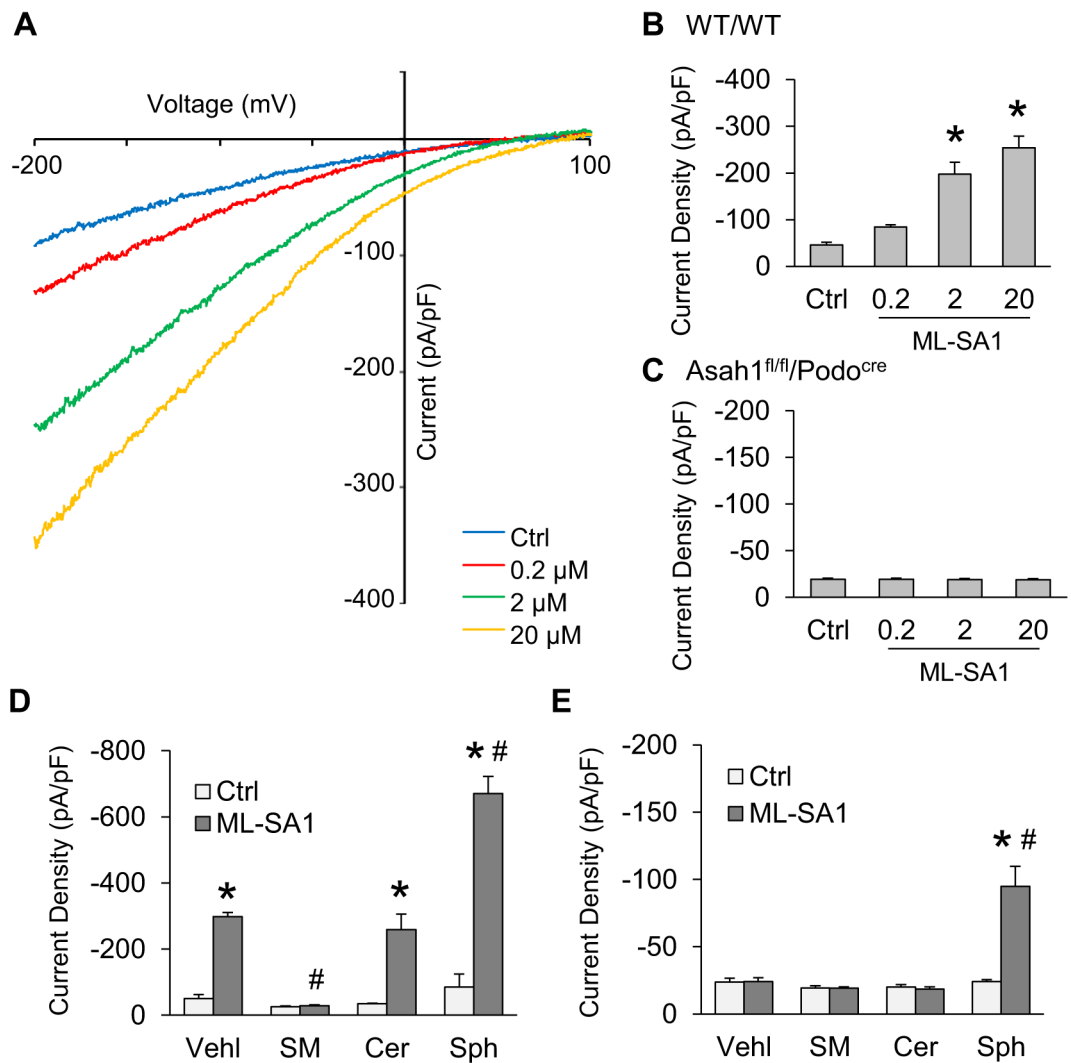
Fig. 6.
Role of different sphingolipids in regulation of TRPML1 channel activity. A. Representative whole lysosome currents enhanced by ML-SA1 in different doses. B. ML-SA1 enhanced TRPML1 channel activity of lysosomes isolated from podocytes of WT/WT mice in a concentration-dependent manner ($n = 5$). C. ML-SA1 failed to enhance TRPML1 channel activity of lysosomes isolated from podocytes of Asah1$^{fl/fl}$/Podo^{cre} mice (n = 6). D. Summarized data of the effects of various sphingolipids on whole lysosome currents of lysosomes isolated from podocytes of WT/WT mice ($n = 3–5$). E. Summarized data of the effects of various sphingolipids on whole lysosome currents of lysosomes isolated from podocytes of Asah1$^{fl/fl}$/Podo^{cre} mice (n = 4–6). *p < 0.05 vs. Ctrl group, #p < 0.05 vs. Vehl group. Ctrl, control; Vehl, vehicle; SM, sphingomyelin; Cer, C16 ceramide; Sph, sphingosine.
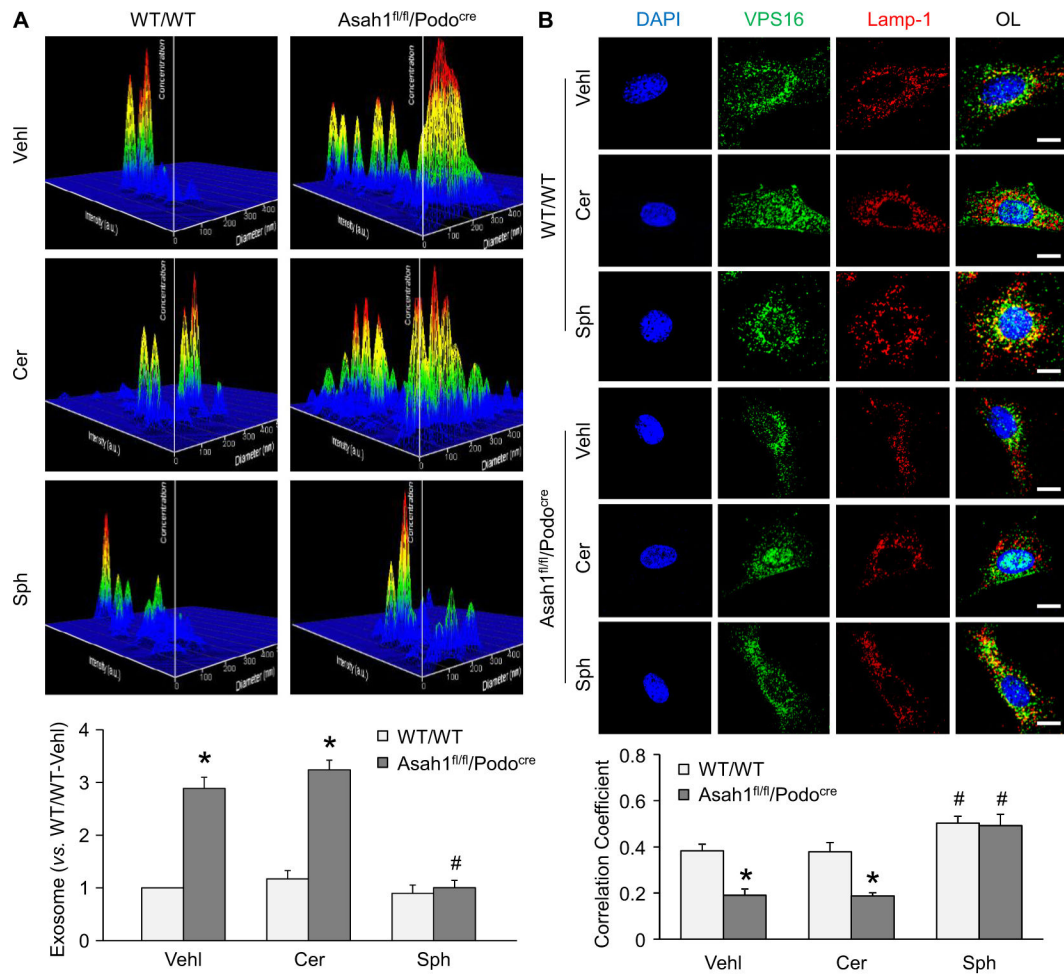
Fig. 7.

Inhibition of exosome release by enhancement of TRPML1 channel activity. A. Representative images and summarized data showing that Sph (10 μM) but not Cer (10 μM) remarkably inhibited exosome secretion from podocytes of Asah1$^{fl/fl}$/Podo^{cre} mice (n = 6–8). B. Representative images and summarized data showing that Sph but not Cer significantly enhanced lysosome-MVB interaction in podocytes lacking Asah1 gene (n = 5–9). Scale bars = 20 μm. *p < 0.05 vs. WT/WT group, #p < 0.05 vs. Vehl group. Vehl, vehicle; Cer, C2 ceramide; Sph, sphingosine.
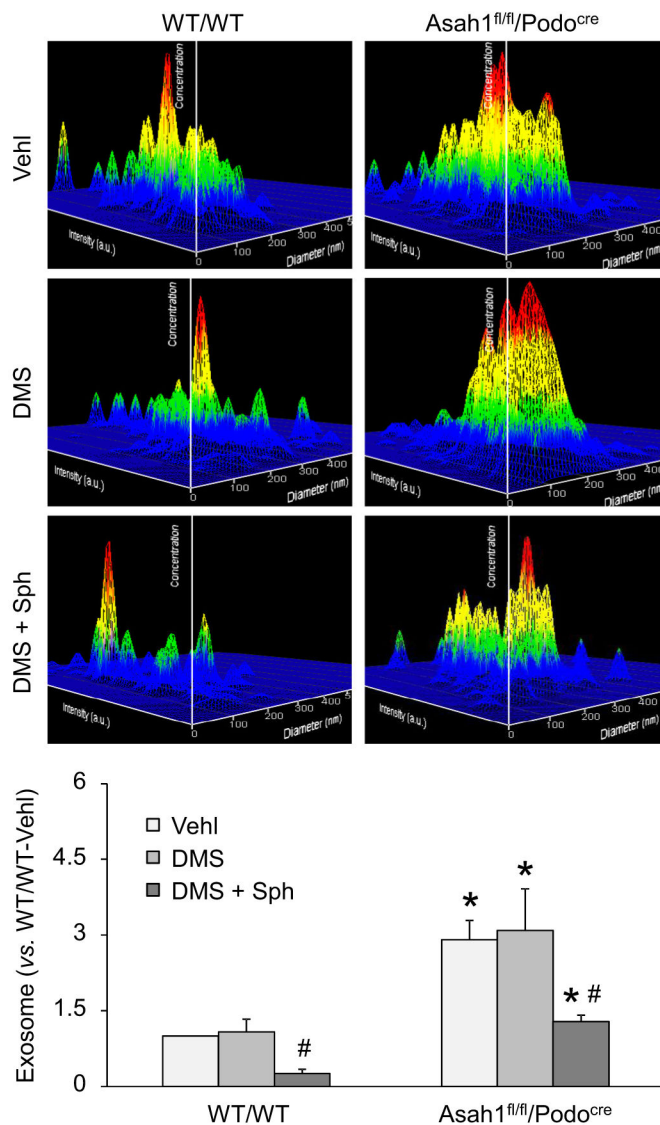
Fig. 8.
Reduction of urinary exosome excretion by Sph. Representative images and summarized data showing that combination of DMS and Sph remarkably inhibited urinary exosome excretion of Asah1$^{fl/fl}$/Podo^{cre} mice. No significant changes of urinary exosome excretion were found between vehicle-treated mice and DMS-treated mice. (n = 3–8). *p < 0.05 vs. WT/WT group, #p < 0.05 vs. Vehl group. Vehl, vehicle; DMS, *N, N*-dimethylsphingosine; Sph, sphingosine.
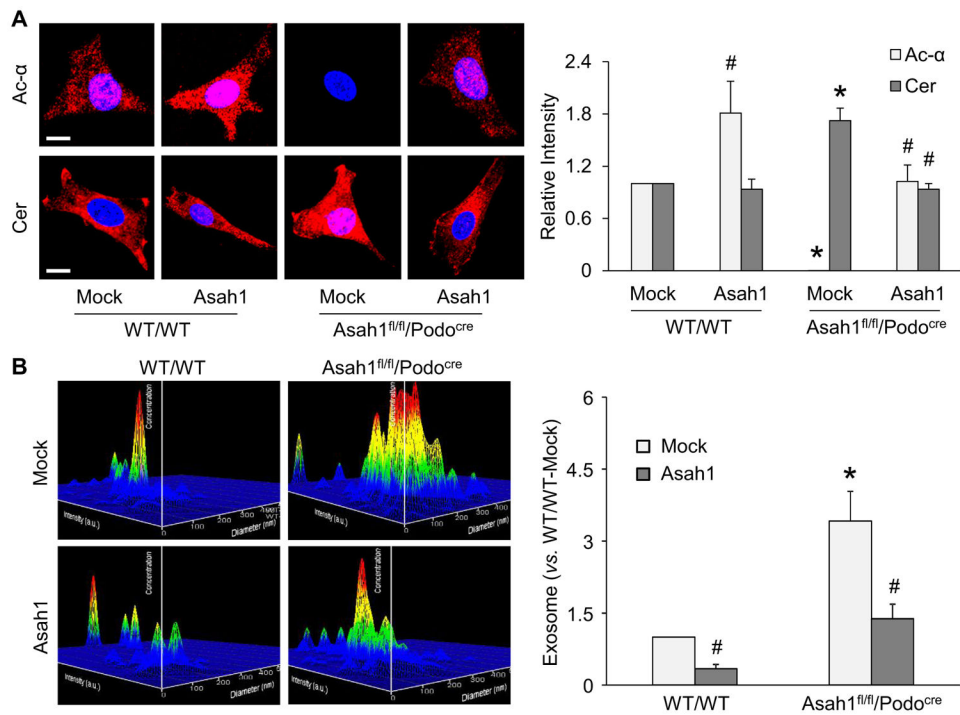
Fig. 9.
Attenuation of exosome release from podocytes of Asah1$^{fl/fl}$/Podo^{cre} mice after rescue of Asah1 gene. A. Representative images and summarized data showing that rescue of Asah1 gene recovered ceramide metabolism in podocytes of Asah1$^{fl/fl}$/Podo^{cre} mice (n = 4–5). Scale bars = 20 μm. B. Representative images and summarized data showing that rescue of Asah1 gene remarkably inhibited exosome secretion from podocytes of Asah1$^{fl/fl}$/Podo^{cre} mice (n = 5–6). *$p < 0.05$ vs. WT/WT group, #$p < 0.05$ vs. Mock group. Mock, mock vector; Asah1, podocyte-specific full-length Ac gene expression vector.